Morphological Classification of Galaxies with Different Grayscale Images Using Deep Learning

João Pedro Holanda[1], **Melissa Sales** [1], **Marcus Ferraz** [1], **Roney Santos**[1]

[1]Centro de Ciências da Natureza, Universidade Federal do Piauí (UFPI)
Teresina – PI – Brazil

{joao.holanda, melissacristal, marcusvinyfz}@ufpi.edu.br,roneyleft@gmail.com

Abstract. *In recent years, several images of galaxies have been collected by telescopes, so that they could be morphologically analyzed using artificial intelligence devices. Thus, this work aims to analyze new image processing approaches, using grayscale conversion algorithms, in order to explore their influence on CNN (Convolutional Neural Networks). Images from the Galaxies10 DECals dataset of two different types of galaxies were used, which were grayscaled and analyzed separately on the CNN. Aspects such as the influence of redshift and the average pixel value have been studied, since grayscale conversions depend on the influence of each channel. It was concluded that, besides altering the assertiveness of the CNN, the applied grayscales also facilitate recognition by the CNN in specific cases.*

1. Introduction

The cosmos is mostly empty space, the occasional lumps of matter and the radiation and gravitational forces that permeate it make a stimulating and interesting environment. Most detectable matter exists as galaxies, which are often clustered together. The boundaries of groups of galaxies occupy about 5% of the volume of space [Elmegreen 1998]. Galaxies are important for understanding the history of the universe, some were formed in the first billion year with traces of the Big Bang, helping to answer cosmological questions and to think about how things will move into the future.

Edwin Hubble was the first to categorize galaxies in a comprehensive way. He classified the galaxies he saw into four basic types—spirals, barred spirals, ellipticals, and irregulars—solely on the basis of their visual appearance [Chaisson et al. 2005]. This classification is known as morphological, started by Hubble's observations at Mount Wilson, later receiving more information from images made by Allan Sandage at Mount Palomar and Las Campanas, respectively in the United States and Chile. [Elmegreen 1998] affirms that this system has been widely adopted because it turns out to be a division of galaxies according to very different compositions, mass distributions, and kinematics.

Visual classification is an incredible time-consuming task. This is an enormous disadvantage in the era of big data, when extremely large surveys release images for millions of galaxies. Visual classification does become a real impossible task [Domínguez Sánchez et al. 2018]. Astronomical surveys such as the Sloan Digital Sky Survey (SDSS) [Eisenstein et al. 2011] and Dark Energy Survey (DES) [Abbott et al. 2018] work with large amounts of images, requiring the voluntary assistance of people for their analysis, thus opening the margin for the use of agile methods present in Artificial Intelligence (AI).

Convolutional Neural Networks (CNN) are considered among the best methods to classify images without the need to extract structural features with high accuracy [Vázquez-Mata et al. 2020]. CNN is an algorithm belonging to Deep Learning, which has as its main characteristic the inspiration in the biological neuron, with its structure containing input signals, characterised by images, which bring with them information about the analysed situation, subsequently coming into contact with the synaptic weights, calculated in the neuron, generating an activation function responsible for producing an output in response to the mapped problem.

The main reason why grayscale representations are often used for extracting descriptors instead of operating on color images directly is that grayscale simplifies the algorithm and reduces computational requirements [Kanan and Cottrell 2012]. A colour image has three conventional channels, commonly called RGB (Red, Green, Blue), the amount of pixels is defined by multiplying the height and width by the channels, so a colour image contains more pixels, while a gray image only works with one channel, reducing the pixels and the neurons in the input layer of the network.

In this work, we used CNN to analyse the prediction in galaxies classification, providing the network inputs with pre-processed grayscale images, checking their correlation with the distance parameter to the galaxies, called redshift (z), and the amount of information in the pixels of the channels.

2. Theoretical Reference

2.1. Galaxies

Around the 18th century, various scientists, specifically astrophysicists, observed among the stars the presence of extensive and diffuse bodies, which were called nebulae. Today, we can identify that different types of objects were grouped together in this initial one, most of which even belong to our own galaxy. Examples of such objects are: gas clouds illuminated by stars within them, gas shells ejected by stars in the final stages of stellar evolution, and star clusters. However, some of these nebulae were also individual galaxies, such as the Milky Way itself.

The first speculations about other galaxies were made by the astronomer Thomas Wright [Oliveira Filho and Saraiva 2004], when in 1750, he wrote a book called "One Original Theory of the Universe" [Wright 2014], where he presented a model explaining the Milky Way as a consequence of being immersed in a locally flat layer of stars and wondered about the existence of other similar galaxies. By the beginning of the last century, approximately 15,000 nebulae had been catalogued and described. Some identified as star clusters and others as gas nebulae. However, the nature of most of them remained unexplained, and one of the biggest problems was the lack of knowledge of the distance to them, which made it impossible to know if they belonged to the Milky Way or not.

In the mid-1920s, Edwin Powell Hubble was able to identify variable Cepheid stars in the Andromeda "nebulae" (M31), which are characterized as young stars that have a periodic variation in brightness over time. It was found, therefore, that the brightness of the new stars found followed the same pattern of variability as those present in the Milky Way. Thus, assuming that all of them followed the known relationship between distance and luminosity, which indicates that stars with short periods of variation in light have

small absolute luminosities [Mitchell 1976], Hubble was able to calculate the distance to Andromeda, obtaining the value of 1 million light-years (this information has now been changed to 2.2 million light-years). However, even though the calculation at the time was not accurate, it served to show that Andromeda was far beyond the boundary of the Milky Way, which is 100,000 light-years across. In other words, Andromeda was an independent star system [Hubble 1926].

In view of this, galaxies are quite different from each other, but most have more regular shapes, making it possible to classify them into spirals, barred spirals, and ellipticals. Also, when they have irregular shapes, they are classified as irregular. As mentioned before, Hubble was the first to use such a classification method, which is still used today. Hubble's scheme cites only the first three classes and treats irregular galaxies as a fourth class of objects, as shown in Figure 1.

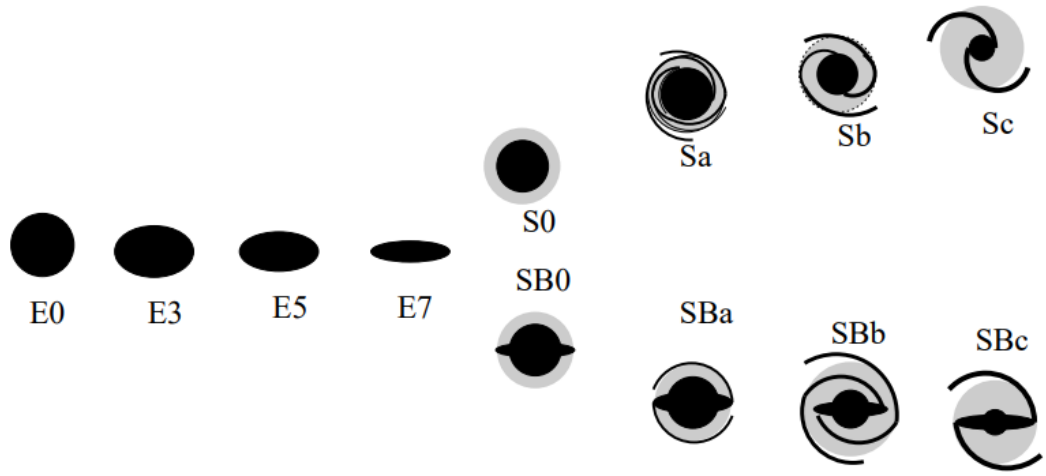

Figure 1. Hubble's scheme for the classification of galaxies.

Starting with the first type of galaxies, the spiral ones, from a frontal view they have a spiral structure - as the name implies. Examples of this are M31 and the Milky Way. Such galaxies have a nucleus, a halo, a disk, and spiral arms. In addition, this category has subdivisions, because the elements of the group can differ due to the size of the core and the degree of development of the spiral arms. Therefore, we have the subgroups: Sa, Sb, Sc, where, from a to c we have an crescent order of the arms, so at a we have the smaller and more coiled arms and at c the larger and more open arms. Conversely, in the same interval we have an inverse variation of size of cores, so from a to c we have a descending order of cores, so the core at a is larger than the core at c.

On the other hand, there are galaxies that have a core, halo, and disk but no trace of spiral structure. These, in Figure 1, are classified as $S0$. These kind of galaxies, together with spirals, form the set of discoidal galaxies. About half of the discoidal galaxies have a bar-shaped structure that runs through the nucleus. They were called barred spirals, or simply SB, by Hubble. As before, this class is separated into subgroups, which are $SB0$, SBa, SBb, and SBc. The arms are a very important feature in this class, because in them it is possible to observe interstellar material, as well as gaseous nebulae, dust and young stars. Finally, these galaxies have diameters ranging from 20,000 light-years to more than

100,000 light-years, and in addition, their masses range up to 10 trillion times the mass of the Sun.

Elliptical galaxies, the third form characterized by Hubble, have a spherical or ellipsoidal shape - as the name implies, and have no spiral structure. In addition, they have a small presence of gas, little dust, and few young stars. The only points in common with spiral galaxies is the presence of a nucleus and a halo. As can be seen in Hubble's scheme shown in Figure 1, the scientist subdivided them from $E0$ to $E7$, according to their degree of flattening. Similar to imagining a circular dish viewed from the front, this would be the shape of an $E0$ galaxy, and as the dish is tilted back and appears elliptical, the number n next to E gradually increases. It is important to note that this classification is based on the appearance of the galaxies and not on their actual shape, that is, it depends on the referential in which the object is being observed. Finally, elliptical galaxies vary in size from dwarfs to super giants.

The last class of galaxies classified by Hubble were the irregular galaxies, which have no circular or rotational symmetry, and thus have a chaotic or irregular structure. Their appearance is dominated by bright young stars and ionized gas distributed without following a pattern. The two best known examples of irregular galaxies are the Large and Small Magellanic Clouds [Oliveira Filho and Saraiva 2004], which are the closest neighboring galaxies to the Milky Way.

2.2. The CNNs to classify images

The CNNs, as a type of neural network, has its modeling inspired by the visual cortex so that it is directly related to Deep Learning. Focused on image classification, Convolutional Neural Networks consist of the input of an image and the output of the classification or apparent probability of belonging to a given class. So, as we are used to classifying things on a daily basis, we might think that it is a relatively simple task, which does not apply to machines.

An image is interpreted as a matrix whose entries can correspond to all positive integers below 256 in the RGB spectrum, resulting in three layers. So if the image is in grayscale, CNN interprets these 3 channels and their given rows and columns as a tensor of order 2 [Wu 2017]. Furthermore, one can just interpret a tensor only as a multidimensional array.

The image used goes through processing belonging to each existing layer in the CNN in order to classify the image. Thus, some examples of layers are: pooling, fully connected layers and convolution layers. In this context, most of the processing occurs in the initial layers and they are the most important ones [Brandão et al. 2005], the last layers are called loss layers [Wu 2017]. In parallel, the loss function used to classify images consists of:

$$H(p,q) = -\sum_{x} p(x) log[q(x)] \tag{1}$$

where the predicted distribution is given by q and the existing one by p.

Thus, convolutional layers rely on a number N of filters, with values said to be "weights" that are adjusted as the network minimizes cost function. In this context, filters can be small matrices on the 3 channels (R, G and B) where real numbers are contained that will be convoluted together with the input data to obtain the characteristic map. Thus,

one can understand the feature map as the convolution between a vector x which is the input of the convolutional layer and y called the kernel. Thus, one can write the convolution as:

$$\zeta = x * y \rightarrow \zeta[j] = \sum_{k=i}^{N} x[j-k]y[k] \tag{2}$$

where i vary according to the apparent need.

Usually to accurately calculate the sum 2 one takes the two vectors shown as filled with zeros, whose ζ becomes infinity filled with several zeros.

2.3. Redshift

Redshift is a very important phenomenon in astrophysics, and its use allows one to begin to understand the characteristics of the Milky Way as a whole. This phenomenon occurs when the electromagnetic radiation emitted or reflected from an object is shifted to the less energetic part of the spectrum (a shorter wavelength) [Gray and Dunning-Davies 2008]. The theories concerning cosmological redshift emerged around the 19th century, with the development of wave mechanics and explorations of the Doppler Effect, a wave phenomenon referring to the apparent change in frequency of a wave when there is relative motion. The first Doppler redshift was described around 1848, when a change in the spectral lines seen in stars was identified. Later, optical redshift was identified by analyzing the solar rotation [Reber 1995].

Subsequently, Hubble discovered a relationship between redshift and Hubble's Law, so that it became evident that the redshift correlated to the light from a distant star is proportional to its distance [Hubble 1929]. If a source of light is moving away from an observer, then a redshift can be observed, conversely, if a source of light is moving toward an observer, a "blueshift" is observed. If the source moves away from the observer with velocity v, then, ignoring relativistic effects, the redshift is given by:

$$z \approx \frac{v}{c} \tag{3}$$

Where c is the speed of light in a vacuum. However, for a more complete understanding of the effect, one must consider the relativistic effects associated with the motion of sources near the speed of light. This "relativistic Doppler effect" describes the total difference in the observed frequencies. The revised expression for redshift is:

$$1 + z = (1 + \frac{v}{c})\gamma \tag{4}$$

Where γ is the factor that expresses the kinematic effect of time-varying dilation.
Therefore, the application of Hubble's idea that the speed at which galaxies move away is proportional to their distances, and that because of this the waves emitted by them suffer a greater redshift, since it is directly proportional to the speed of the emitting body, proved this conception. In this context, it is known that the recession velocity, such that H_0 is called Hubble's constant:

$$\chi = H_0 r \tag{5}$$

The result found by Hubble was the first notion that the universe is not static.

2.4. Grayscale

Modern descriptor-based image recognition systems often operate on grayscale images [Kanan and Cottrell 2012]. Currently there are a considerable number of algorithms to convert images to grayscale, some of them use weighted equations in the RGB channels, others apply corrections for a more accurate perception, among other methodologies.

Following the notation used by [Kanan and Cottrell 2012], for algorithms with linear time complexity, a function $\mathcal{G}$, which use a colour image represented by $\mathrm{R}^{\mathrm{n}\times\mathrm{m}\times 3}$, and end as $\mathrm{R}^{\mathrm{n}\times\mathrm{m}}$. Where RGB represents the linear channels, and (RGB)' represents the gamma correction channels, defined by function $\Gamma(t) = t' = t^{1/\gamma}$, which performs a brightness adjustment on the image.

The Intensity algorithm is given by the average of the channels:

$$\mathcal{G}_{Intensity} = \frac{1}{3}(R + G + B) \tag{6}$$

Gleam has the same equation as Intensity, but with gamma correction applied:

$$\mathcal{G}_{Gleam} = \frac{1}{3}(R' + G' + B') \tag{7}$$

Trying to follow the brightness perception of the human eye, Luminance is given by the following equation:

$$\mathcal{G}_{Luminance} = 0.3R + 0.59G + 0.11B \tag{8}$$

Luma is an algorithm used in the grayscale conversion of commercial applications, having similarity with the gamma correction used in last generation televisions:

$$\mathcal{G}_{Luma} = 0.2126R' + 0.7152G' + 0.0722B' \tag{9}$$

There are several other methods of grayscale conversion (Lightness, Value, Luster, etc), using different equations, expressing the amount of possible information that can be obtained, depending on which algorithm is used.

3. Related Work

According to [Yamauchi et al. 2005], as cited by [Cardoso et al. 2021], with the advance of digital surveys and the consequent increase in the amount of data collected, it is important to develop fast and automated methods for the morphological classification of galaxies with the accuracy of the traditional visual classification performed by humans.

[Domínguez Sánchez et al. 2018] proposed an CNN using the Keras library [Ketkar 2017] for the Python programming language, being able to classify the SDSS-DR7 dataset [Abazajian et al. 2009], where it contains 670,000 images, presenting average accuracy above 97% in the developed models. Using previous CNN models, similar to those previously developed by Sánchez, [Vázquez-Mata et al. 2020] managed to perform the separation of 4,600 galaxies, between ellipticals and spirals, from the data survey of Mapping Nearby Galaxies at Apache Point Observatory (MaNGA), being used

the grayscale for display in pre-processing, in order to identify possible structures in the region of the nucleus, reaching 96% accuracy to separate early from late type galaxies and 60% for the multiclass classification.

In order to test the efficiency of the algorithms used in everyday cases, it was found some CNN models already implemented and consolidated, in order to test the efficiency of the algorithms used in everyday cases, which mostly use images with characteristics different from those found in astronomy, in this way, Zhu et al. [Zhu et al. 2019] created a network with 26 layers, merging its architecture with Residual Neural Networks (ResNet), coming from the challenges of visual recognition. Following the same direction, [Cardoso et al. 2021] proposed in their work the comparison of ResNet using images from S-PLUS, obtaining promising results, demonstrating that the transfer of learning has an important role, acting in general cases of classification.

[Silva and Ventura 2019], in the pre-processing part, imposed a method used by [Perez and Wang 2017], known as Data Augmentation, in order to generalize the network, producing 10,000 extra images with distinct rotations and mirroring, besides added zoom in the images to focus on the galaxies, excluding the interference of stars in their neighborhood. In the preparation of the CNN, the choice of the approaches applied on the set of images is a crucial factor. [Kanan and Cottrell 2012] present a study with linear and non-linear methods of conversion to grayscale, explaining their influence on the performance of visual recognition of people and objects, recommending that the conversion methods should be indicated in all scientific publications, a fact that is not usually common.

The study about the use of conversion to grayscale proposed in this project is pertinent. The characteristics of the channels in the composition of RGB images applied to monochromatic tones aims to detect regions with structures of predominant brightness in galaxies, in search of new approaches that direct the pre-processing phase of the CNN.

4. Method

4.1. Data

The Galaxies10 DECals [Walmsley et al. 2022] is a dataset formed by ten classes, containing 17,736 color images composed by the G, R and Z bands, corresponding to the three channels. Its images have dimensions of 256x256 pixels, besides, the dataset has information of coordinates and redshift of galaxies.

Using supervised learning concepts, each image has its respective class within the dataset. For this research a binary sample was created with two classes, separated between Barred Spiral and Round Smooth galaxies, with 500 for each class, accounting for a total of 1,000 images in Portable Network Graphics (PNG) format, that were used on CNN. The proportion of data splitting was done with 80% for training and 20% for testing.

All images were subjected to grayscale pre-processing, as can be seen in Figure 2, using the equations shown in Section 2.4, with the y-value of 0.5 for channels with gamma correction, generating 4,000 images, which were used separately in the CNN, following their respective conversion algorithms.

4.2. Model

The architecture chosen for CNN was LeNet-5 [LeCun et al. 1998], as can be seen in Figure 3, being composed of two convolution layers with different numbers of filters (6

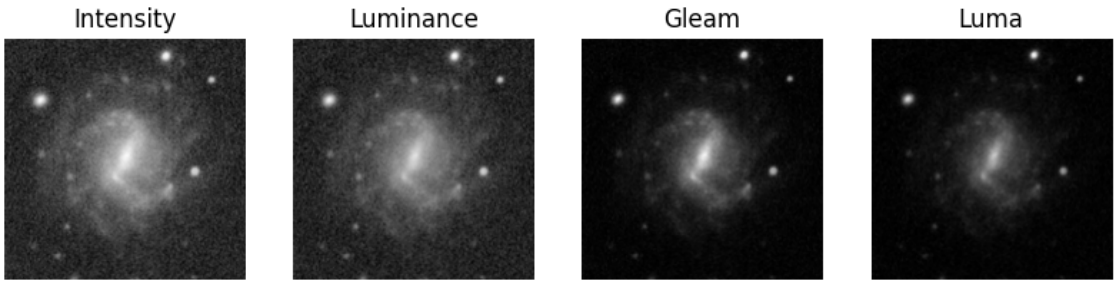

Figure 2. Pre-processed grayscale Barred Spiral galaxy.

and 16, respectively) and average pooling, followed by a flatten layer with 120 feature maps, entering a fully connected dense layer, changing from Relu to Softmax activation function in the output layer.

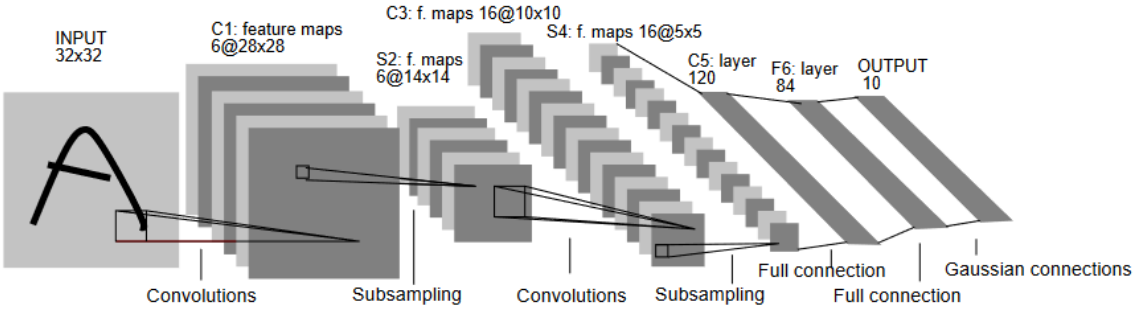

Figure 3. LeNet-5 Architecture.

The difference between the original LeNet-5 architecture and the one used in this work refers to the quantity of neurons in the output layer, with a decrease from ten to two, motivated by the binary dataset created. Furthermore, in the input layer, the dimensions of the images were modified, since the images present in Galaxies10 DECals are larger than the original handwritten digits used in the LeNet-5 dataset, not being applied resizing processing in the images.

In the preprocessing of the images, the regularization technique Data Augmentation [Wang et al. 2017] was used, where the images are underwent rotation, flip and zoomed, based on the work of [Domínguez Sánchez et al. 2018]. Consisting of generating new instances of images from those arranged in the dataset, in order to increase the training set, escaping from overfitting.

5. Results and Discuss

Before starting the training and testing of the network, an Exploratory Data Analysis (EDA) was performed with the dataset features. A near redshift was found, with approximately 0.15, as seen in the Figure 4 .

Another explored characteristic of the images was the mean pixel values, since the conversions to the grayscale depend on the influence of each channel. It can be noticed in the Figure 5, a similarity in the intervals of each channel, in this case independently of the equation used for the conversion, the coefficients will have a relevant importance.

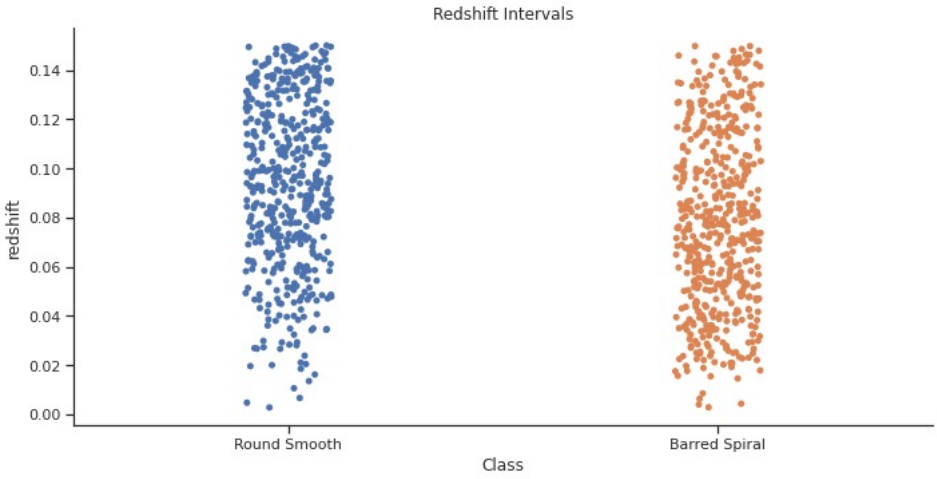

Figure 4. Redshift range in dataset.

This analysis is relevant, because if there was a great disparity in the image channels, the conversion results would be different in the same algorithm.

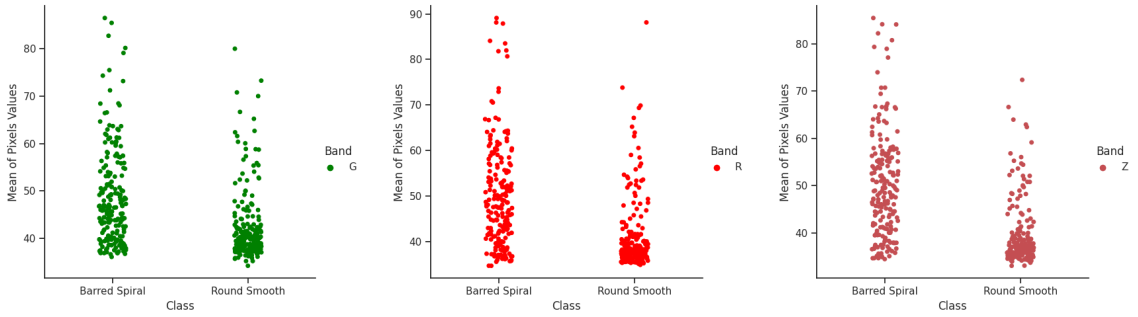

(a) G Band. **(b) R Band.** **(c) Z Band.**

Figure 5. Mean of pixels values in each images channels.

In a empiric way, we set the CNN training epochs to 50, which demonstrated a visible difference in performance as seen in Figure 6. The CNN that received the images pre-processed with the Intensity algorithm obtained the worst values of accuracy and loss, while the images with the Luminance algorithm obtained a regular performance, and the best results were with Gleam and Luma, with the last mentioned algorithm obtaining a slightly better value in the metrics.

In the test set with images not yet seen by CNN, the loss explained in Section 2.2 with equation 1, and the accuracy, which aims at analyzing the assertiveness rate of the model following the confusion matrix, given by equation:

$$Accuracy = \frac{True\ Positive\ (TP) + True\ Negative\ (TN)}{Total} \tag{10}$$

obtained values close to those achieved in training, as seen in Table 1. Luma takes a slight advantage compared to Gleam, 92.5% against 91% accuracy, right behind comes Luminance with its 87%, the last place was occupied by Intensity with 75.5%.

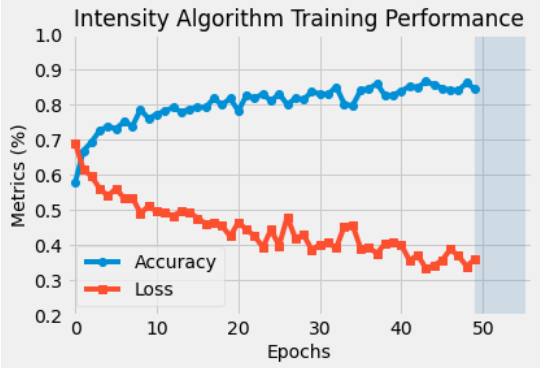

(a) Intensity

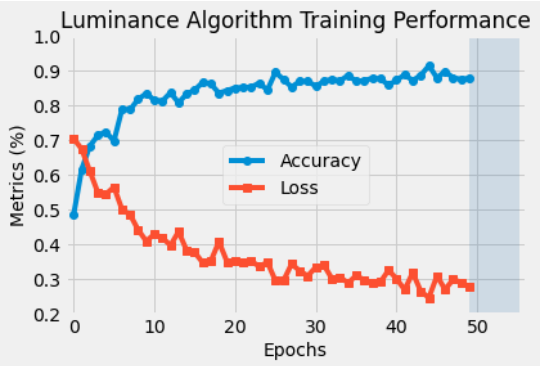

(b) Luminance

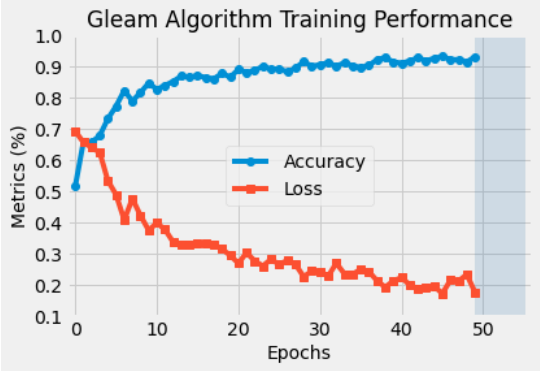

(c) Gleam

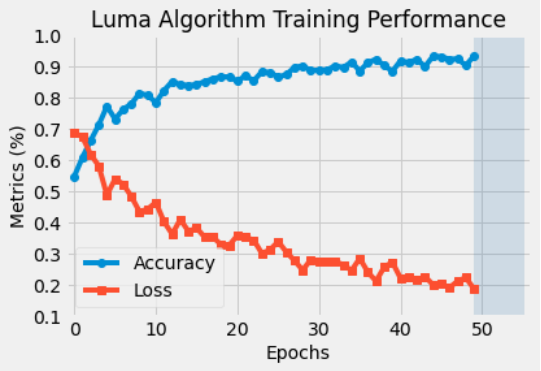

(d) Luma

Figure 6. CNN training performance with different images inputs.

Grayscale Images	Accuracy	Loss
Intensity	0.755	0.481
Luminance	0.870	0.301
Gleam	0.910	0.184
Luma	0.925	0.190

Table 1. Accuracy and Loss of the CNN in test set.

For each separate class of galaxies, verification of the Precision, Recall and F1-Score metrics was performed. The Precision is focused on the results classified as positive, exclusively on the true positives, expressed by the equation:

$$Precision = \frac{True\ Positive\ (TP)}{True\ Positive\ (TP) + False\ Positive\ (FP)} \tag{11}$$

Recall has as concept the correct classification when viewed a sample in the dataset, for example, how many spiral galaxies the model saw and classified correctly. This metric is given by:

$$Recall = \frac{True\ Positive\ (TP)}{True\ Positive\ (TP) + False\ Negative\ (FN)} \tag{12}$$

F1-Score merges Precision and Recall, seeking a generalization rate of the model

that indicates its quality, as seen in the following equation:

$$F1 - Score = \frac{2 \times Precision \times Recall}{Precision + Recall} \tag{13}$$

Class	Precision	Recall	F1-score
Barred Spiral	0.95	0.54	0.69
Round Smooth	0.68	0.97	0.80

(a) Intensity

Class	Precision	Recall	F1-score
Barred Spiral	0.97	0.76	0.85
Round Smooth	0.80	0.98	0.88

(b) Luminance

Class	Precision	Recall	F1-score
Barred Spiral	0.99	0.83	0.90
Round Smooth	0.85	0.99	0.92

(c) Gleam

Class	Precision	Recall	F1-score
Barred Spiral	0.94	0.91	0.92
Round Smooth	0.91	0.94	0.93

(d) Luma

Table 2. CNN metrics in each class.

In Table 2, it can be seen that the model with the Luma images has balanced values for precision and recall, achieving the best generalization. In Gleam grayscale, the Barred Spiral galaxies obtained a high precision in their classification, while the Round Smooth galaxies had a good performance in their recognition. The CNN with Luminance and Intensity images in its input layer, mixed distinct precision and recall results, with its overall performance being impaired.

A constant factor is seen in the results of the metrics in all models, is that the Barred Spiral galaxies always achieve a higher precision value, while the Round Smooth have a higher recall rate. This is due to the fact that the structure of the spirals are visibly more predominant, as the Round Smooth have a well-defined shape, providing a greater recall, since the spirals suffer from arms that may be visibly fainter or the nucleus of the galaxy with more brigthness.

The distance of the galaxy does not seem to be a determining factor in the classification. The dataset consisted of galaxies with near redshift, containing images with good quality, if they were distant galaxies it could be affected by the fainter brightness. So, it is possible to see in Figure 7 the errors in the whole redshift range of the dataset. In addition, most of the errors are arranged in Barred Spirals, due to the previously discussed facts regarding brightness and arms, as well as other celestial bodies in the vicinity of the central galaxy that confuse the algorithm.

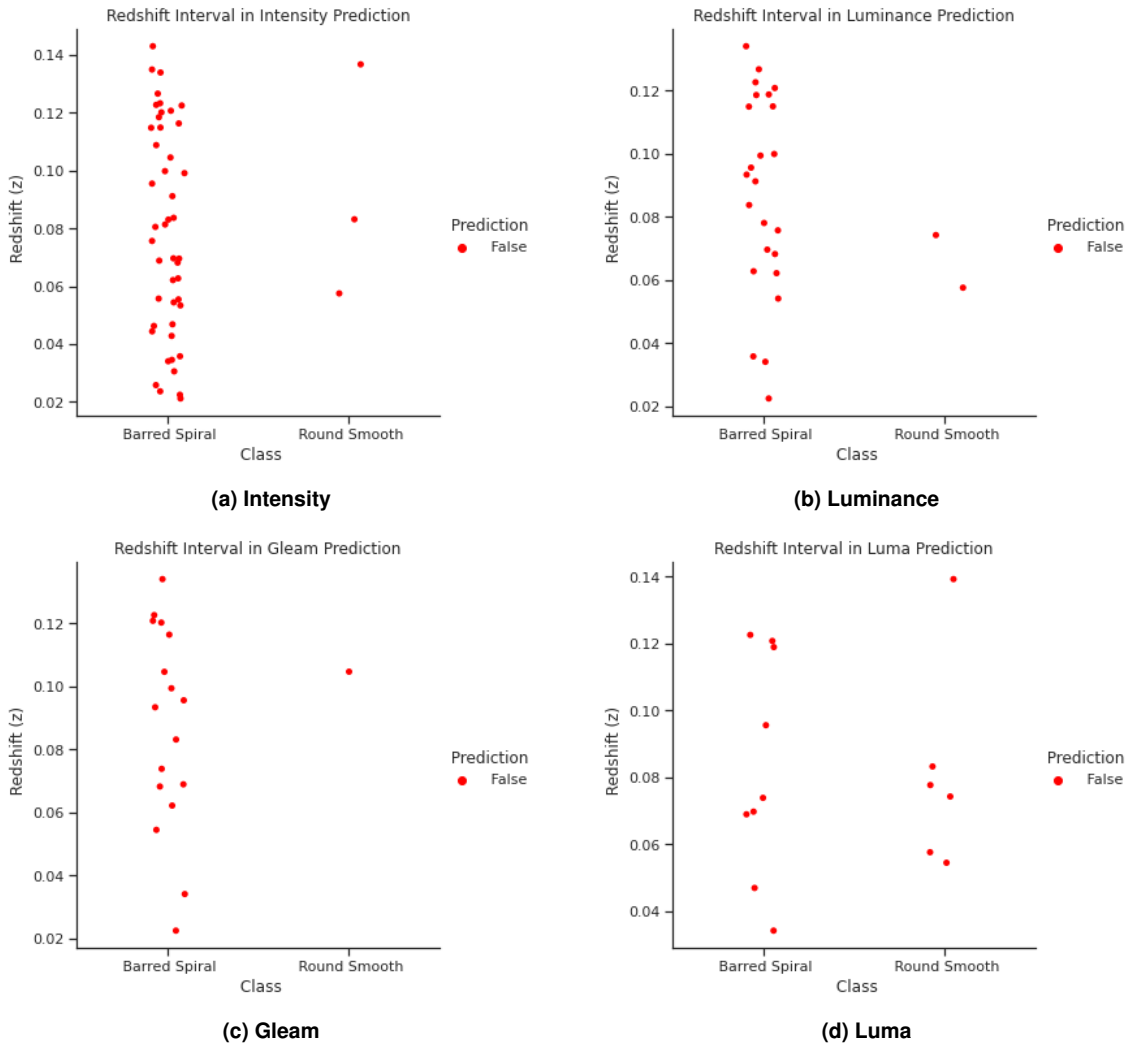

(a) Intensity **(b) Luminance**

(c) Gleam **(d) Luma**

Figure 7. Redshift false prediction interval.

6. Conclusion

In this work, we present the morphological classification of 1,000 galaxies from the Galaxy10 DECals dataset, subjected to pre-processing in grayscale, seeking to analyze its effectiveness in image recognition in the astronomical environment. In order to achieve the results obtained, algorithms known as CNNs were used. Galaxies images of the Barred Spiral and Round Smooth classes were used to train and test the model using LeNet-5, a CNN architecture consolidated in the in the area of computer vision.

Analyzing the results, it is possible to notice that the grayscale applied in the galaxies images alters the percentage of assertiveness of the CNN, especially the models that received images with gamma correction, because they highlight the structure of the predominant galaxy, omitting other objects in its neighborhood, taking advantage in relation to the images that use the three linear channels without alteration. In the case of grayscale conversions without gamma correction, it is noticeable that the weighted equation assigned to Luminance, which approximates human perception, works better than the average of the channels seen in Intensity, facilitating recognition by CNN.

Moreover, for the classification of the galaxies, at a near redshift, the distance to the galaxies was not a determining factor, because the images were of good quality, not compromising the performance of the algorithm. The results obtained were close to the state of the art, presenting good results compared to consolidated models found in the literature, shown in Section 3. It is an alternative to be explored to reduce computational resources and processing time, opening the possibility of use in unsupervised approaches, given the optimistic numbers achieved with different grayscale.

In future research, improvements can be made by increasing the dataset going from binary to multi-classification, providing a more arduous task for the algorithm in the face of new classes of galaxies added. Also, other grayscale can be used, to observe if there might be better approaches that positively grow the metrics found in the results. Finally, other CNNs architectures (ResNet) and approaches (Transfer Learning) used in Deep Learning can be applied.

Acknowledgments

The authors are grateful to FAPEPI (Fundação de Amparo à Pesquisa do Estado do Piauí) for supporting this work.

References

Abazajian, K. N., Adelman-McCarthy, J. K., Agüeros, M. A., Allam, S. S., Prieto, C. A., An, D., Anderson, K. S., Anderson, S. F., Annis, J., Bahcall, N. A., et al. (2009). The seventh data release of the sloan digital sky survey. *The Astrophysical Journal Supplement Series*, 182(2):543.

Abbott, T., Abdalla, F., Allam, S., Amara, A., Annis, J., Asorey, J., Avila, S., Ballester, O., Banerji, M., Barkhouse, W., et al. (2018). The dark energy survey: Data release 1. *The Astrophysical Journal Supplement Series*, 239(2):18.

Brandão, A. S., Pizziolo, T. A. O., Souza, R. N. O., and Faria, M. N. (2005). Redes neurais artificiais aplicadas ao reconhecimento de comandos de voz. *Trabalho de Conclusão de Curso. Engenharia Elétrica, Universidade Federal de Viçosa–UFV–2005*.

Cardoso, N. C., Schwarz, G. O., Dias, L. D., Bom, C. B., Sodré Jr, L., and Oliveira, C. M. (2021). Classificação morfológica de galáxias no s-plus por combinação de redes convolucionais. *NOTAS TÉCNICAS*, 11(2).

Chaisson, E., McMillan, S., and Rice, E. (2005). *Astronomy today*. Pearson/Prentice Hall Upper Saddle River, NJ.

Domínguez Sánchez, H., Huertas-Company, M., Bernardi, M., Tuccillo, D., and Fischer, J. (2018). Improving galaxy morphologies for sdss with deep learning. *Monthly Notices of the Royal Astronomical Society*, 476(3):3661–3676.

Eisenstein, D. J., Weinberg, D. H., Agol, E., Aihara, H., Prieto, C. A., Anderson, S. F., Arns, J. A., Aubourg, É., Bailey, S., Balbinot, E., et al. (2011). Sdss-iii: Massive spectroscopic surveys of the distant universe, the milky way, and extra-solar planetary systems. *The Astronomical Journal*, 142(3):72.

Elmegreen, D. M. (1998). *Galaxies and galactic structure*. New Jersey: Prentice Hall.

Gray, R. and Dunning-Davies, J. (2008). A review of redshift and its interpretation in cosmology and astrophysics. *arXiv preprint arXiv:0806.4085*.

Hubble, E. (1929). A relation between distance and radial velocity among extra-galactic nebulae. *Proceedings of the national academy of sciences*, 15(3):168–173.

Hubble, E. P. (1926). Extragalactic nebulae. *Astrophysical Journal, 64, 321-369 (1926)*, 64.

Kanan, C. and Cottrell, G. W. (2012). Color-to-grayscale: does the method matter in image recognition? *PloS one*, 7(1):e29740.

Ketkar, N. (2017). Introduction to keras. *Deep learning with python: a hands-on introduction*, pages 97–111.

LeCun, Y., Bottou, L., Bengio, Y., and Haffner, P. (1998). Gradient-based learning applied to document recognition. *Proceedings of the IEEE*, 86(11):2278–2324.

Mitchell, H. B. (1976). Henrietta swan leavitt and cepheid variables. *The Physics Teacher*, 14(3):162–167.

Oliveira Filho, K. d. S. and Saraiva, M. d. F. O. (2004). Astronomia e astrofısica. *Rio Grande do Sul: Livraria da Fısica*.

Perez, L. and Wang, J. (2017). The effectiveness of data augmentation in image classification using deep learning. *arXiv preprint arXiv:1712.04621*.

Reber, G. (1995). Intergalactic plasma. *Astrophysics and Space Science*, 227:93–96.

Silva, M. and Ventura, T. (2019). Classificaçao morfológica de galáxias por meio de redes neurais. In *Anais da X Escola Regional de Informática de Mato Grosso*, pages 31–36. SBC.

Vázquez-Mata, J. A., Hernandez-Toledo, H. M., and Mascherpa, L. C. (2020). Galaxy Morphology classification using CNN. In *Proceedings of Artificial Intelligence for Science, Industry and Society — PoS(AISIS2019)*, volume 372, page 006.

Walmsley, M., Lintott, C., Géron, T., Kruk, S., Krawczyk, C., Willett, K. W., Bamford, S., Kelvin, L. S., Fortson, L., Gal, Y., et al. (2022). Galaxy zoo decals: Detailed visual morphology measurements from volunteers and deep learning for 314 000 galaxies. *Monthly Notices of the Royal Astronomical Society*, 509(3):3966–3988.

Wang, J., Perez, L., et al. (2017). The effectiveness of data augmentation in image classification using deep learning. *Convolutional Neural Networks Vis. Recognit*, 11(2017):1–8.

Wright, T. (2014). *An Original Theory or New Hypothesis of the Universe, Founded upon the Laws of Nature*. Cambridge University Press.

Wu, J. (2017). Introduction to convolutional neural networks. *National Key Lab for Novel Software Technology. Nanjing University. China*, 5(23):495.

Yamauchi, C., Ichikawa, S.-i., Doi, M., Yasuda, N., Yagi, M., Fukugita, M., Okamura, S., Nakamura, O., Sekiguchi, M., and Goto, T. (2005). Morphological classification of galaxies using photometric parameters: The concentration index versus the coarseness parameter. *The Astronomical Journal*, 130(4):1545.

Zhu, X.-P., Dai, J.-M., Bian, C.-J., Chen, Y., Chen, S., and Hu, C. (2019). Galaxy morphology classification with deep convolutional neural networks. *Astrophysics and Space Science*, 364:1–15.